characterized the relatively stable alkene compounds (η^2-*trans*-cyclooct)Fe(CO)(NO)$_2$ and (η^2-*trans*-cyclooct)$_2$Fe(NO)$_2$ (cyclooct = cyclooctene), and Table III compares the appropriate frequencies.

After prolonged UV photolysis of Fe(CO)$_2$(NO)$_2$ and 1-butene, all of the Fe(CO)$_2$(NO)$_2$ was destroyed and its ν(C-O) and ν(N-O) bands disappeared from the IR spectrum (Figure 5b). In the absence of these bands of Fe(CO)$_2$(NO)$_2$, the ν(N-O) bands of both photoproducts, colored black in Figure 5b, are easily seen. Most surprisingly, however, Figure 5b also reveals that the ν(C-O) absorption of Fe(CO)(NO)$_2$(η^2-1-btn) is a *doublet*, which on closer inspection has traces of an additional shoulder, marked with an asterisk in Figure 5c. These bands are all due to the same compound, and their relative intensities change reversibly as the solution is warmed. Such band splittings are unusual but are not unprecedented in organometallic compounds. A particularly striking example is the splitting of the a′ ν(C-O) mode of (η^6-C$_6$H$_5$X)Cr(CO)$_3$ compounds,[22] which may be due to different rotamers. Similarly, in the present case the splitting of the ν(C-O) mode of Fe(CO)(NO)$_2$(η^2-1-btn) appears to be due to different conformers of the coordinated 1-butene. This explanation is also consistent with the more detailed analysis of the bands of coordinated 1-butene (see the supplementary material).

Prolonged UV photolysis also resulted in the formation of a reddish solid, insoluble in LXe. It was presumably a polynuclear compound, but unfortunately the amount of material was too small for characterization.

Thermal Stabilities of Fe(CO)(NO)$_2$(η^2-1-btn) and Fe(NO)$_2$(η^2-1-btn)$_2$. There is no evidence for thermal decay of either butene complex on standing for 1 h at -104 °C. However, when the cell is warmed up to -55 °C, the bands assigned to the disubstituted species decayed rapidly ($t_{1/2} \simeq$ 2min). At the same time, there were clear and reproducible increases in the intensities of the ν(^{13}C-O) bands of Fe(CO)(NO)$_2$(η^2-1-btn) and the ν(C=C) band of uncoordinated butene and a decrease in the absorption of due to free CO in the solution. These changes are consistent with the reaction

$$\mathrm{Fe(NO)_2(\eta^2\text{-}1\text{-}btn)_2 + CO \xrightarrow{LXe} Fe(CO)(NO)_2(\eta^2\text{-}1\text{-}btn) + 1\text{-}btn}$$

The rate of this thermal decay is substantially reduced by increasing the concentration of free butene in solution. This observation would be consistent with a dissociative mechanism. However, since the unsubstituted nitrosyl-carbonyl compounds are known to react thermally by both associative and dissociative pathways,[23] it would be unwise to speculate on the mechanism of the thermal decay without further evidence.

In contrast with the thermal decay of Fe(NO)$_2$(η^2-1-btn)$_2$, both Fe(CO)(NO)$_2$(η^2-1-btn) and Co(CO)$_2$(NO)(1-btn) showed no evidence of thermal decay even at -30 °C, the highest temperature currently attainable in our cell. The thermal instability of the disubstituted iron nitrosyl compound is reminiscent of our earlier experiments[4] with N$_2$ ligands, where Fe(NO)$_2$(N$_2$)$_2$ was thermally much less stable than Fe(CO)(NO)$_2$(N$_2$).

Conclusion

In this paper we have demonstrated that IR spectroscopy is a very sensitive technique for characterizing unstable organometallic compounds dissolved in liquefied xenon. In particular, one can observe IR bands due to vibrations of coordinated organic ligands, bands that would be masked by IR absorptions of more conventional solvents. Even the relatively straightforward reaction with 1-butene has revealed striking differences in behavior between Co(CO)$_3$NO and Fe(CO)$_2$(NO)$_2$. The Fe center can coordinate two olefin molecules, while under similar conditions the Co center can only coordinate one. The difference is suggestive of the greater efficiency of Fe(CO)$_2$(NO)$_2$ as a dimerization catalyst,[10] and we shall discuss this reaction in more detail in a separate paper.[11]

Acknowledgment. We thank the SERC for support. We are grateful to Dr. M. B. Simpson, Dr. M. A. Healy, Dr. J. G. McLaughlin, R. K. Upmacis, and J. G. Gamble for all their help with this work.

Registry No. Co(CO)$_2$(NO)(η^2-1-butene), 103752-18-7; Fe(CO)(NO)$_2$(η^2-1-butene), 103752-19-8; Fe(NO)$_2$(η^2-1-butene)$_2$, 103752-20-1; Co(CO)$_3$NO, 14096-82-3; Fe(CO)$_2$(NO)$_2$, 13682-74-1.

Supplementary Material Available: Harmonic ν(C-O) and ν(N-O) frequencies for Co(CO)$_3$(NO) and Co(CO)$_2$(NO)(η^2-1-btn) (Table IV) and wavenumbers and tentative assignment of the observed IR bands of coordinated and uncoordinated 1-butene (Table V and Figures 6-10) (9 pages). Ordering information is given on any current masthead page.

---

(22) Davidson, G.; Fish, P. V.; Tankard, M., unpublished observations.

(23) Thorsteinson, E. M.; Basolo, F. *Inorg. Chem.* **1966**, *5*, 1691. Basolo, F. *Inorg. Chim. Acta* **1985**, *100*, 33.

Contribution from the Departments of Chemistry, McGill University,
Montreal, Quebec, Canada, and University of Witwatersrand, Johannesburg, South Africa

Solid-State Micro-Raman and Fourier Transform Infrared Spectra of Mixed Carbonyl-Isocyanide Dirhenium(0) Complexes, Re$_2$(CO)$_{10-n}$(CNR)$_n$ (n = 1-4)

Pierre D. Harvey,[1a] Ian S. Butler,*[1a] Gillian W. Harris,[1b] and Neil J. Coville[1b]

Received November 26, 1985

Vibrational assignments are proposed for the solid, mixed carbonyl-isocyanide dirhenium(0) derivatives Re$_2$(CO)$_{10-n}$(CNR)$_n$ (R = Me, *t*-Bu, benzyl, n = 1-3; R = 2,6-xylenyl, n = 1-4), on the basis of their room-temperature micro-Raman and FT-IR spectra. Successive replacement of the CO groups by CNR ligands results in a gradual shift of the ν(CO) modes to lower wavenumbers, while the reverse is observed for the ν(Re-C) modes. These shifts are good indicators of the stronger σ-donor and poorer π-acceptor capacities of the CNR ligands compared to those of CO. Moreover, the shifts increase with changes in R in the order Me < benzyl < *t*-Bu < 2,6-xylenyl, presumably reflecting the increased steric hindrance due to the bulkiness of the R ligands. There is no correlation between the position of the strongest Raman peak at 120 cm^{-1} and the Re-Re bond distances in these mixed carbonyl-isocyanide derivatives, demonstrating that this peak cannot be attributed solely to the ν(Re-Re) mode, as had been suggested previously.

Introduction

Decacarbonyldirhenium(0), Re$_2$(CO)$_{10}$, is a particularly simple example of a metal-metal bonded complex in which two, staggered, square-pyramidal Re(CO)$_5$ fragments are held together by a single Re-Re bond.[2,3] In general, the D_{4d} vibrational selection rules are obeyed for the solid and in solution,[4] but the activity

---

(1) (a) McGill University. (b) University of Witwatersrand.

(2) Dahl, L. F.; Ishishi, E.; Rundle, R. E. *J. Chem. Phys.* **1957**, *26*, 1750-1751.

(3) Churchill, M. R.; Amoh, K. N.; Wasserman, H. J. *Inorg. Chem.* **1981**, *20*, 1609-1611.

0020-1669/86/1325-3608$01.50/0 © 1986 American Chemical Society

of some forbidden modes suggests that the molecule is slightly distorted, in agreement with its X-ray structure. Numerous research groups have been interested in the synthesis and physical properties of substituted binuclear metal complexes containing such metal pairs as MnMn, ReRe, MnRe, CoMn, and CoRe with tertiary phosphines and arsines,[5] silanes,[6] and isocyanides.[7-13] Most recently, the catalyzed CO substitution reactions of $Re_2(CO)_{10}$ with isocyanides (CNR) have received particular attention.[10-13] Previously, only one study had been published on this topic.[7]

Since its discovery in 1941,[14] the IR and Raman spectra of $Re_2(CO)_{10}$ have been investigated extensively,[4] but there has been comparatively little work on the vibrational spectra of the $Re_2(CO)_{10-n}(CNR)_n$ derivatives.[7,10,13] After single-crystal X-ray diffraction, one of the most promising techniques for studying the properties of metal–metal-bonded compounds is Raman spectroscopy.[15] Often, single-crystal measurements prove difficult and Raman spectroscopy provides a useful alternative, especially since reasonable correlations between M–M bond lengths and ν(M–M) exist. For complexes such as $Re_2(CO)_{10-n}L_n$, steric factors (more than electronic ones) induced by the ligands L have a strong influence the M–M bond distances, especially at higher values of n.[12] Not surprisingly, steric effects dominate in the case of bulky ligands, e.g., PMe_2Ph (Tolman cone angle 122°) in *axial*-$Mn_2(CO)_9(PMe_2Ph)$.[16] Unfortunately, many organometallic complexes undergo thermal decomposition under normal laser irradiation and Raman spectra are often unattainable. However, with the recent development of the micro-Raman (or Raman microprobe) technique, this problem may be surmountable because of the rapid heat loss from a microscopic particle upon laser irradiation. Also, lower laser powers are possible because of the extremely efficient collection of the scattered light using a microscope.[17]

In this paper, we report the results of a systematic study of the micro-Raman and FT-IR spectra of a variety of solid $Re_2(CO)_{10-n}(CNR)_n$ complexes. We were particularly interested in measuring the shifts in the bands associated with the Re–Re, Re–CO, Re–CN, CN, and CO stretching modes upon increasing the number of CNR substituents.

Experimental Section

Crystalline $Re_2(CO)_{10}$ (Strem Chemical Co.) was purified immediately prior to use by slow sublimation under vacuum (10^{-3} torr, 80 °C). The $Re_2(CO)_{10-n}(CNR)_n$ complexes were prepared according to the literature procedures.[11-13] The microcrystalline samples were sealed in Pyrex capillaries for the Raman measurements, which were made on an Instruments S.A. Ramanor spectrometer equipped with a U-1000 Jobin-Yvon 1.0-m double monochromator and a Columbia Data Products minicomputer. The instrument was operated in the micro-Raman mode using the 514.5-nm green line of a Spectra Physics Model 164 argon ion laser (10-20 mW at the samples) for excitation. The spectra were calibrated against the emission lines of a standard neon lamp, and the peak positions are considered to be accurate to ±0.2 cm^{-1}. All the FT-IR spectra were recorded on a Nicolet Model 6000 spectrometer using a liquid-nitrogen-cooled, mercury-cadmium telluride detector (accuracy ±0.2 cm^{-1}).

Results and Discussion

The parent $Re_2(CO)_{10}$ complex has eight equatorial carbonyls and two axial ones—its Raman spectrum in the 2200–2220-cm^{-1} region is shown in Figure 1 (supplementary material). The totally symmetric CO stretching mode for the axial carbonyls appears at 1976 cm^{-1}, while that for the equatorial carbonyls is at 2125 cm^{-1}. Similarly, the totally symmetric Re–CO stretching modes are at 473 and 458 cm^{-1}, but these cannot be classified as purely axial or equatorial because they are extensively mixed. The highest intensity peak at 120 cm^{-1} has been the subject of much controversy. It was originally assigned to the Re–Re stretch, but subsequent single-crystal Raman polarization and IR reflectance experiments,[18,19] as well as Raman data for $Re_2(CO)_8Cl_2$ (for which no Re–Re bond exists[20]), have contradicted this suggestion. In the following analysis, the bands due the CO, CN, Re–CO, and Re–CN stretching modes and the 120-cm^{-1} peak will be used as probes of the effect of replacement of CO by CNR. The observed micro-Raman and FT-IR bands, together with the proposed assignments, for the methyl isocyanide derivatives are given in Table I. Similar data for the other complexes are presented in the supplementary material (Tables II–IV).

Methyl Isocyanide Derivatives. Of all the known isocyanides, methyl isocyanide ($CNCH_3$) is certainly the most investigated, and vibrational spectra of the neat liquid have been reported by several groups.[21] Also, detailed potential-function and normal-coordinate calculations have been published.[22,23] From the vibrational data listed in Table I for the $Re_2(CO)_{10-n}(CNCH_3)_n$ (n = 1–3) complexes, the perturbations caused by complexation of the $CNCH_3$ ligands are especially evident in the ν(CN) region.

The free $CNCH_3$ ligand has a ν(CN) mode at 2162 cm^{-1}, whereas $\nu(CN)_{sym}$ for the complexed isocyanide occurs at 2235 ± 5 cm^{-1}.[24] There are also some slight changes for the rest of the $CNCH_3$ frequencies (free ligand, complexed ligand): 3011, 3005 ± 5; 2959, 2953 ± 3; 1460, 1445 ± 3; 1422, 1415/1410; 1129, 1119 ± 2; 280, 308 ± 1 cm^{-1}. The N–C(H)$_3$ stretching modes are unfortunately obscured owing to the large number of bands in the 1000–900-cm^{-1} region. There is no particular trend for the methyl isocyanide frequencies with increasing substitution. In the Raman spectra, the ν(Re–CN) modes appear at about 380 cm^{-1}. The differences in frequencies between the free and complexed ligand may be explained by changes in the resonance structures shown.[25]

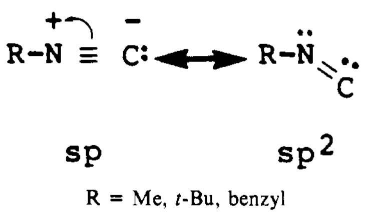

R = Me, *t*-Bu, benzyl

The linear isocyanide has a higher "s" character located at the ternary carbon atom and exhibits a CN triple bond (having pseudo

---

(4) Harvey, P. D.; Butler, I. S. *Can. J. Chem.* **1985**, *63*, 1510–1517 and references therein.
(5) See, for example: Fawcett, J. P.; Poe, A. J.; Twigg, M. V. *J. Organomet. Chem.* **1973**, *61*, 315–321.
(6) See, for example: Cowie, M.; Bennett, M. J. *Inorg. Chem.* **1972**, *16*, 1556–1561.
(7) Prasad, P. N. *Spectrochim. Acta* **1977**, *33A*, 335–339.
(8) Adams, R. D.; Chodosh, D. F. *J. Organomet. Chem.* **1975**, *87*, C48–C51.
(9) Albers, M. O.; Coville, N. J. *S. Afr. J. Chem.* **1982**, *35*, 139–145.
(10) Robinson, D. J.; Harris, G. W.; Boeyens, J. C. A.; Coville, N. J. *J. Chem. Soc., Chem. Commun.* **1984**, 1307–1308.
(11) Albers, M. O.; Boeyens, J. C. A.; Coville, N. J.; Harris, G. W. *J. Organomet. Chem.* **1984**, *260*, 99–104.
(12) Harris, G. W.; Boeyens, J. C. A.; Coville, N. J. *Organometallics* **1985**, *4*, 914–922.
(13) Harris, G. W.; Coville, N. J. *Organometallics* **1985**, *4*, 908–914.
(14) Hieber, W.; Fuchs, H. *Z. Anorg. Chem.* **1941**, *248*, 256–268.
(15) Lee, S. W.; Wang, L. F.; Cheng, C. P. *J. Organomet. Chem.* **1982**, *236*, 213–219.
(16) Laing, M.; Singleton, E.; Reimann, R. *J. Organomet. Chem.* **1973**, *56*, C21–C22.
(17) Harvey, P. D.; Butler, I. S. *Microbeam Analysis 1985*; Armstrong, J. A., Ed.; San Francisco Press: San Francisco, CA, 1985; pp 49–53.
(18) Adams, D. M.; Hooper, M. A. *J. Organomet. Chem.* **1979**, *181*, 131–141.
(19) Adams, D. M.; Taylor, I. D. *J. Chem. Soc., Faraday Trans.* **1982**, *78*, 1065–1090.
(20) Swanson, B. I.; Rafalko, J. J.; Shriver, D. F.; San Filippo, J., Jr.; Spiro, T. G. *Inorg. Chem.* **1975**, *14*, 1737–1738.
(21) See, for example: Davies, J. E. D.; Wood, W. J. *J. Raman Spectrosc.* **1973**, *1*, 383–385 and references therein.
(22) Duncan, J. L.; McKean, D. C.; Mackenzie, M. W.; Perez Pena, J. *J. Mol. Spectrosc.* **1979**, *76*, 55–70.
(23) Nicolaisen, F. M.; Hansen, J. S. *Mol. Phys.* **1982**, *47*, 1265–1275.
(24) Several other bands appear at lower energy for the n = 1 complexes that are due to antisymmetric ν(CN) modes. These modes are more intense than those for the free ligands.
(25) Howell, J. A. S.; Saillard, J.-Y.; LeBeuze, A.; Jaouen, G. *J. Chem. Soc., Dalton Trans.* **1982**, 2533–2537.

Table I. Vibrational Spectra (cm^{-1}) and Proposed Assignments for the $Re_2(CO)_{10-n}(CNMe)_n$ Complexes (n = 1–4)

n = 1		n = 2		n = 3		n = 4	
FT-IR	Raman	FT-IR	Raman	FT-IR	Raman	FT-IR	assignments
	3000 vw, br	2995 vw, sh	3011 w, br	3000 sh, w	3012 w	3000 w, sh	
2965 sh	2966 sh	2965 sh	2970 sh		2955 sh	2957 sh	
2950 w	2952 w	2952 w	2955 m	2946 w	2949 m	2943 sh	ν(CH)
2932 sh		2931 sh					
2921 w		2922 w		2923 sh		2924 m	
2898 sh		2898 sh			2893 vw	2899 sh	
2872 w		2870 w	2874 w	2872 w	2877 w	2868 w	overtones
2852 w		2852 w		2853 sh		2850 w	
		2800 vw		2802 w	2802 w		
2233 sh		2237 sh	2241 w	2838 sh	2234 w	2229 sh	
2215 m	2208 m	2215 s	2209 s	2206 s	2007 s	2208 vs	
2207 sh		2198 s	2198 s	2189 s	2181 s		ν(CN)$_{eq}$
						2173 vs	
		2167 sh	2172 sh	2171 sh	2070 sh	2140 sh	
						2040 s	
	2130	2082 sh		2082 sh			
				2070 m	2068 w		
2103 s	2105 m	2069 s	2067 m	2040 s	2044 m	2022 sh	
						1993 vs	
2073 s	2056 m	2023 s	2028 m	2027 s		1973 sh	
2050 s	2048 m					1954 vs	
	2029 m		2006 w			1927 sh	
2018 sh	2015 m	1994 sh	1997 w			1914 vs	
2000 vs	1996 m		1982 m	1985 vs	1988 m	1896 vs	ν(CO)
1985 sh	1988 m	1977 vs	1974 sh				
	1979 m	1968 vs	1967 m	1964 sh	1967	1857 vs	
1972 vs	1971 m	1944 vs	1949 m	1944 vs	1945 ± 5 sh	1736 m	
1960 sh	1962 m						
	1955 m	1920 vs	1920 s	1918 vs	1920 m		
1946 vs	1948 m		1905 m	1908 vs	1903 m		
1936 vs	1930 m	1883 sh	1895 sh	1894 vs	1891 sh		
1926 vs	1919 m						
1443 w	1448	1444 w	1445 vw	1444 w	1445	1442 m	
1413 w	1414 w	1416 w	1416 w	1412 w	1416 m	1408 s	
1409 w	1410 w	1409 sh	1409 w		1410 m	1404 sh	CH_3 deformations
1384 vw		1384 vw				1384 vw	
1263 vw		1263 vw				1278 sh	
						1262 m	
				1168 w			
1147 vw		1159 w		1155 w			
1117 vw		1120 w		1121 w		1119 w	CH_3 rock
						1099 w	
1088 vw	1085 vw	1078 w	1087 vw	1078 w	1077 vw	1073 w	
						1047 w,	
1042 vw		1038 w		1024 w		1037 w	
						1027 w	
1008 vw	1009 vw	1005 w	1000 vw	977 w	977 vw		overtones and combinations of Re–CO region
				950 sh			
970 w	972 vw	973 w	973 w				
935 vw				920 w			
912 vw		907 vw		907 w		909 w	
	881 vw		879 vw				
863 vw	860 vs, sh		863 vw				
806 vw	800 vw	803 vw	820 vw			816 sh	
						802 w	
613 sh	613 w	609 sh	610 w		611 w	616 sh	Re–CO bending (π)
603 sh	603 w	599 s		603 s		608 vs	
592 sh	591 w		590 sh				
587 s	581 w	580 s	586 w	580 s	586 w		Re–CO bending (δ)
580 s					575 w	578 s	
					564 w		
547 m	548 m				550 sh	551 sh	
538 m	541 m	542 s	545 w	534 s	541 m	539 m	Re–CO bending (π)
						534 m	
505 m	503 m		497 w	499 m	500 sh	502 m	Re–CO bending (δ)
	491 m				493 m	495	
480 m	481 m	480 m	480 sh	482 m		482 m	ax + eq ν(Re–CO)
	463 s		465 s		467 s		
458 m				361 m		461 m	ν(Re–CO)
447 m	450 m	455 m	455 sh				
439 m		439 m		435 m	435 w		ax Re–CO bending
431 m	430 sh						
399 s	403 sh	407 s	401 m	407 m	406 sh	416 w	eq ν(Re–CO)
395 sh	394 m	401 s		401 m	403 m		
	378 w		378 w		380 w		ν(Re–CN)

Table I (Continued)

n = 1		n = 2		n = 3		n = 4	
FT-IR	Raman	FT-IR	Raman	FT-IR	Raman	FT-IR	assignments
	308 vw		308 vw		307 w		CNC bending
	184 w		184 vw				overtones + combinations?
	139 sh		130 sh				CReC bending (π)
	120 vs		114 vs		116 vs		CReC bending + ν(Re–Re)
	111 sh		103 sh		105 sh		
	97 sh		97 sh		95 sh		CReC bending (π)
	87 s		85 sh		85 sh		
	79 sh		79 sh				
68 m		64 m		68 s			torsion
55 sh		54 s					ν_L
47 sh		45 s		41 s			ν_L
41 vs		34 vs					translatory modes
33 s		28 sh		24 s			
19 s		20 s					

Table V. Position of $\nu(CO)_{eq}$ (cm^{-1}) for the $Re_2(CO)_{10-n}(CNR)_n$ Complexes as a Function of n

R	$\nu(CO)_{eq}$ $n = 0$	$n = 1$	$n = 2$	$n = 3$	$n = 4$
t-Bu	2125	2096	2058	2027	
2,6-$C_6H_3Me_2$		2093	2058	2034	1973
$PhCH_2$		2103	2067	2036	
Me		2105	2068	2043	burns

"sp" hybridization), causing the CN stretching frequency to be at higher energy than that for the bent structure. Increasing the electron density at the nitrogen atom by shifting the equilibrium toward the linear structure will increase the CN stretching and CNC bending frequencies, while the CH stretching and CH_3 bending modes will decrease slightly in energy. The structure of $Re_2(CO)_7(CNCH_3)_3$ has been determined recently: $P2_1/n$, $Z = 4$, with two $CNCH_3$ ligands occupying cis-equatorial positions on one Re atom and the third $CNCH_3$ ligand on the other Re atom disordered with respect to the carbonyl trans to it.[12] The average CNC angle in the $CNCH_3$ ligands is 173.2 (19)°, indicating a slight distortion from linearity.

***tert*-Butyl Isocyanide Derivatives.** The only vibrational frequency reported for CNBu-t is the CN stretching mode (2137 cm^{-1} in CCl_4 solution).[26] Again, there is a substantial increase in ν(CN) upon coordination. The IR spectra show a peak at ~2181 cm^{-1} for $Re_2(CO)_{10-n}(CNBu\text{-}t)_n$ where $n = 1$ and 2, but not for $n = 3$. The highest energy ν(CN) Raman band is at 2175 ± 1 cm^{-1} for this series of complexes. The $Re_2(CO)_9(CNBu\text{-}t)$ complex crystallizes in the $Pbca$ ($D_{2h}{}^{15}$) space group with eight molecules per unit cell. The CNC angle is 175.7 (18)°, indicating essentially linear geometry for the CNBu-t ligand. The CN stretching region for this complex does not show any evidence of factor group splitting with one band in the IR (2181 cm^{-1}) and the Raman (2176 cm^{-1}) spectra. However, the ν(CO) region is quite complicated due to some correlation splitting with 14 Raman and 11 IR peaks being observed. For eight molecules per unit cell located at C_1 sites, under D_{2h} factor group symmetry, the nine ν(CO) modes (6a′ + 3a″) for the isolated molecule should theoretically give rise to 36 Raman ($9a_g + 9b_{1g} + 9b_{2g} + 9b_{3g}$) and 27 IR ($9b_{1u} + 9b_{2u} + 9b_{3u}$) frequencies if the full factor group splittings could be detected.

In general, the group frequencies of the CNBu-t ligand are well characterized in the three derivatives, especially in the ν(C–H) region. The ν(C–N) and ν(C–C) modes are more difficult to identify in the solid state for $n = 1$ and 2. In the IR spectra, these modes are weak and are hidden among weak overtones and combinations of the Re–C stretching and ReCO bending modes. Except for the 435 ± 5, 393, and 335 ± 1 cm^{-1} peaks, the vibrational spectra below 650 cm^{-1} are characteristic of the $Re_2(CO)_{10-n}$ moieties. The symmetric Re–CN stretch is easily assigned to 405 cm^{-1} because of the gradual increase in intensity with the extent of substituion (Figure 2). In contrast to the $CNCH_3$ complexes, very few combination and overtone bands are observed in the Raman spectra of the solid CNBu-t complexes.

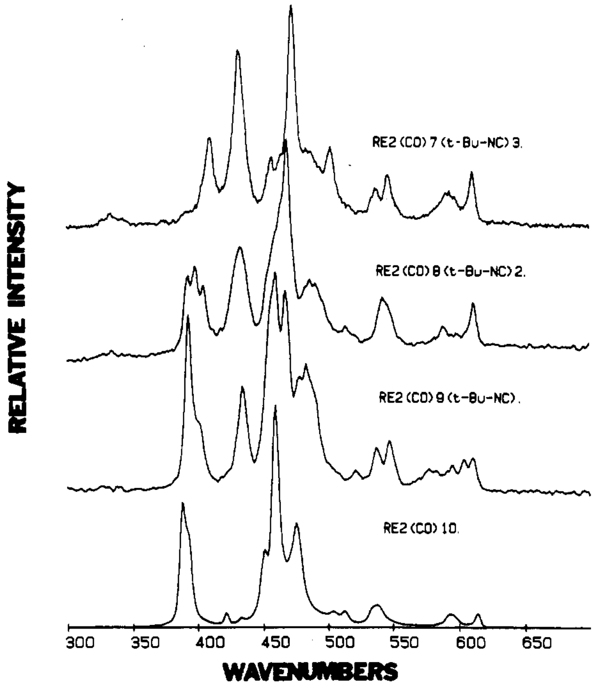

Figure 2. Micro-Raman spectra of solid $Re_2(CO)_{10-n}(CNBu\text{-}t)_n$ complexes (n = 0–3) at room temperature in the 300–700-cm^{-1} region. Laser excitation: 514.5 nm (30 mW at sample); slits 100 μm; data points spaced by 1 cm^{-1} (4 s point^{-1}); 2 scans; no smoothing or base line correction; 32× microscope objective.

Benzyl Isocyanide Derivatives. Surprisingly, the vibrational frequencies of the free $CNCH_2Ph$ ligand have apparently never been reported in the literature, although the IR spectrum is available in the Aldrich Library (IR 3,1140D). Table III (supplementary material) lists the IR data for the neat liquid at room temperature. The same peaks also appear clearly in the vibrational spectra of the $Re_2(CO)_{10-n}(CNCH_2Ph)_n$ (n = 1–3) complexes. The proposed vibrational assignments for the ligand modes, both when in the free state and when coordinated, are based on those for benzene and methylene,[27,28] e.g., ca. 696 cm^{-1} (Ph CCC deformation), ca. 1190 cm^{-1} (Ph CCH in-plane bending), ca. 1330 cm^{-1} (methylene CH wag), ca. 1440 cm^{-1} (methylene CH scissor).

The ν(CN) region for the $Re_2(CO)_{10-n}(CNCH_2Ph)_n$ derivatives increases in complexity with increased substitution of CO by

---

(26) Harris, D. C.; Bertolucci, M. D. *Symmetry and Spectroscopy*; Oxford University Press: New York, NY, 1978; p 202.

(27) Painter, P. C.; Coleman, M. M.; Koenig, J. L. *The Theory of Vibrational Spectroscoy and its Application to Polymeric Materials*; Wiley-Interscience: New York, NY, 1982; p 165.

(28) Colthup, N. B.; Dody, L. H.; Wiberly, S. E. *Introduction to Infrared and Raman Spectroscopy*; Academic: New York, NY, 1975; pp 259, 323.

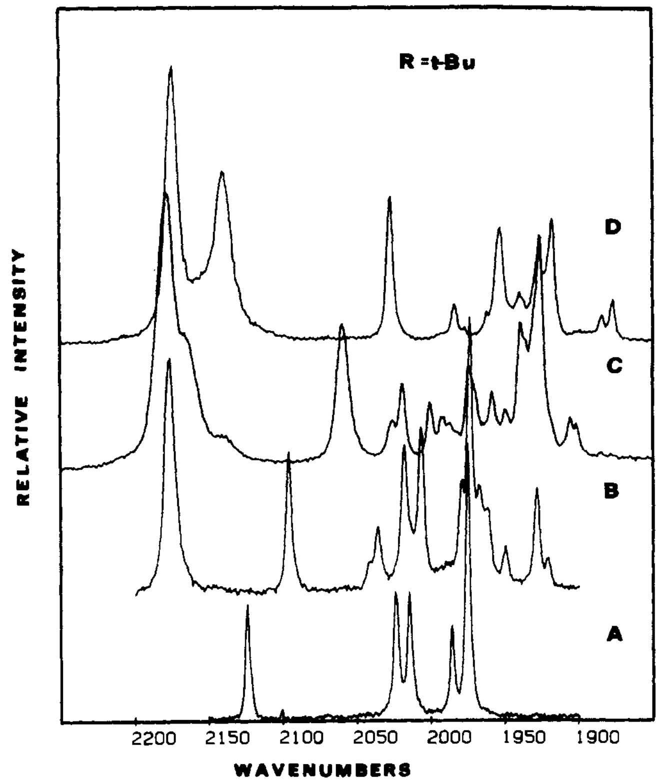

Figure 3. Micro-Raman spectra of solid $Re_2(CO)_{10-n}(CNBu\text{-}t)_n$ complexes (n = 0–3) at room temperature in the 2250–1850-cm^{-1} region: A, n = 0; B, n = 1; C, n = 2; D, n = 3. The same experimental conditions as those in Figure 2 were used except that laser power at the sample was 10–20 mW.

$CNCH_2Ph$: n = 1, 2200 vs (IR) and 2202 s (R) cm^{-1}; n = 2, 2201 vs (IR) and 2196 vs/2184 s/2157 w, sh (R) cm^{-1}; n = 3, 2190 vs/2168 vs/2163 vs/2159 vs (IR) and 2190 vs/2163 s, sh/2153 vs (R) cm^{-1}. The ν(CO) region is complicated for each complex with clear evidence of factor group splitting, and as usual, successive CO substitution results in a gradual shift of the peaks to lower wavenumbers. The ν(Re–CN) modes appear at ca. 380 cm^{-1}. In the case of $Re_2(CO)_7(CNCH_2Ph)_3$, the vibrational data (cm^{-1}) in the ν(CN) and ν(CO) regions are suggestive to a centrosymmetric unit cell because of the lack of coincidences: 2159 (IR) with 2153 (R); 1963 (IR) with 1969 (R); 1954/1937 (IR) with 1949 (R); 1909 (IR) with 1905 (R); 1884 (IR) with 1892 (R). It is possible that this complex is isostructural with $Re_2(CO)_7(CNCH_3)_3$, which crystallizes in the $P2_1/n$ (C_{2h}^2) space group (Z = 4).[12] The Raman spectra of the two complexes are quite similar and are less resolved than those for the related complexes with n = 1 and 2. The tris(methyl isocyanide) complex is disordered such that there are two isomeric forms in the same unit cell, and perhaps it is the superposition of two different band systems that accounts for the poorly resolved Raman spectrum in the ν(CO) region. A similar situation may obtain for $Re_2(CO)_7(CNCH_2Ph)_3$. The other assignments given in Table III are fairly straightforward since the low-energy modes of the $CNCH_2Ph$ ligand are significantly weaker than those of the $Re_2(CO)_{10-n}$ moieties.

2,6-Xylenyl Isocyanide Derivatives. The IR and Raman spectra of the free ligand have never been investigated, but the closely related phenyl isocyanide has been studied.[29,30] With these previous data and those obtained from the FT-IR and micro-Raman spectra of free 2,6-xylenyl isocyanide, vibrational assignments for the complexes can be undertaken with more confidence (see Table IV, supplementary material). Unlike the results for the other isocyanide ligands, many frequencies differ markedly (often by more than 10 cm^{-1}) on going from the free to the complexed ligand, especially for vibrations associated with the C=N—C moiety. For instance, ν(CN) shifts from 2123 cm^{-1} for the free ligand to 2151 ± 4 cm^{-1} for the complexes. The C–CN stretch increases from 1174 to 1186 ± 3 cm^{-1}, while the C=N—C in-plane bend goes from 362 to 335 cm^{-1}. The ligand torsions behave similarly. The observed shifts can be attributed to the following resonance structures:

Some Resonance Structures of the Free Ligand

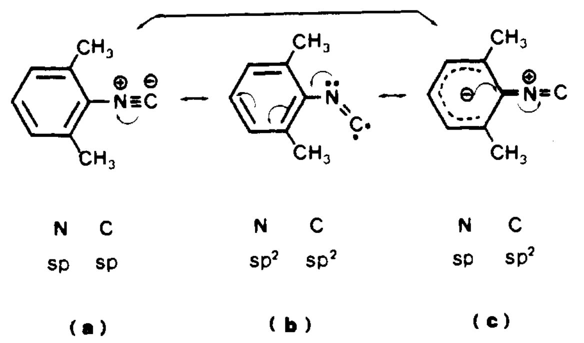

Some Resonance Structures of the Complexed Ligand

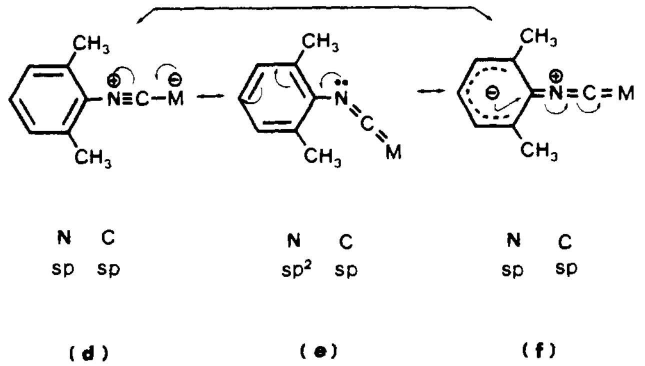

Although the crystal structure of 2,6-xylenyl isocyanide has not been reported, the structures of $Re_2(CO)_8(CNC_6H_3Me_2\text{-}2,6)_2$ and $Re_2(CO)_6(CNC_6H_3Me_2\text{-}2,6)_4$ have just been published.[12] The C=N—C angles in these derivatives are approximately 176–177°. Only resonance structures d and f give such angles. On the other hand, the large difference between the CN stretching vibrations of the free and complexed ligand can only be explained by resonance structures b and c of the free ligand. Finally, because the CN stretching vibration of the free ligand is lower than that of the complexed one, we have to conclude that structure c is improbable. Structure f would be stabilized by the metal atom, while structure e is unlikely because of large steric interactions with the carbonyl groups in the complexes.

The 2250–1850-cm^{-1} Region. The micro-Raman spectra of the solid $Re_2(CO)_{10-n}(CNBu\text{-}t)_n$ complexes in this region are shown in Figure 3; similar spectra for the three other series of isocyanide complexes are given in the supplementary material (Figures 4–6). The band splittings observed in the micro-Raman and FT-IR spectra are related to the decreasing molecular symmetry that occurs with substitution and to solid-state effects (due to unit cell occupancy). $Re_2(CO)_6(CNC_6H_3Me_3\text{-}2,6)_4$ appears to be an exception because its FT-IR spectrum in n-hexane solution displays only three ν(CO) and two ν(CN) peaks,[13] which also seems to be true for the solid, while the Raman spectrum of the solid exhibits four ν(CO) and three ν(CN) bands.

In general, the CO stretching bands shift toward lower energies with increasing CNR substitution. The ν(CN) modes, on the other hand, are not dramatically affected, in accord with the good σ-donor and poor π-acceptor properties of the isocyanide ligands. Table II shows the position of the ν(CO) peak for the equatorial groups. It is clear that, depending on the R group of the isocyanide ligand, the symmetric $\nu(CO)_{eq}$ mode is not exactly the same in each complex. In fact, a systematic trend is observed such that

---

(29) Bak, B.; Kierkegaard, C. *Acta Chem. Scand.* **1973**, *27*, 2531–2535.

(30) Nalepa, R. A.; Laposa, J. D. *J. Mol. Spectrosc.* **1974**, *50*, 106–104.

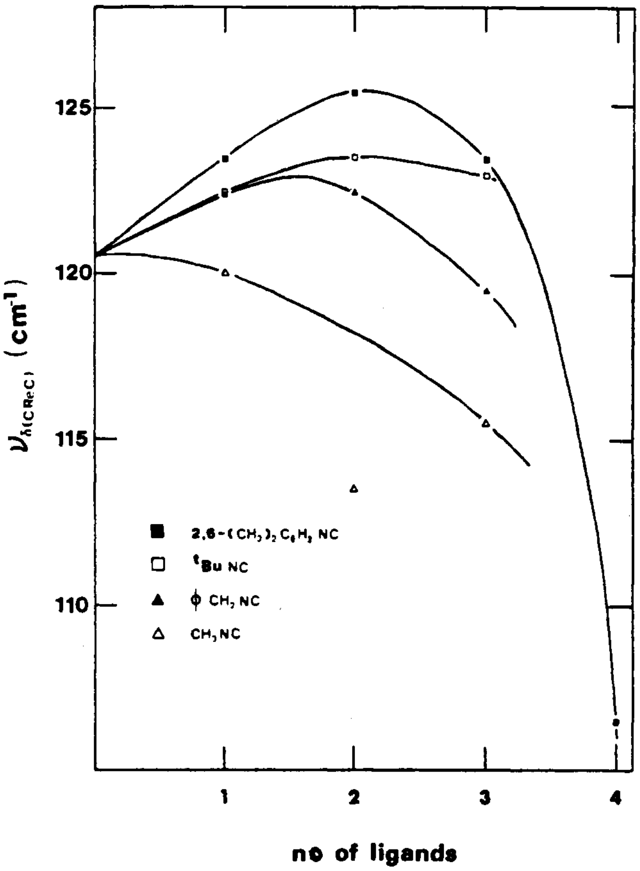

Figure 7. Plot of the position of the δ(CReC) mode in the 120-cm^{-1} region for the $Re_2(CO)_{10-n}(CNR)_n$ complexes vs. n.

regardless of the number of CO groups substituted, $\nu(CO)_{eq}$ shifts with changes in R as Me < benzyl < 2,6-xylenyl < t-Bu. In our attempts to rationalize these observations, the 2,6-xylenyl isocyanide ligand should first be omitted because of its different resonance forms. The trend is clearly related to the steric hindrance associated with the R groups. Interactions between the R groups and the CO ligands in the complexes lead to the C═N—R linkages becoming more linear. The crystal structures that have been reported[12] show clear evidence of the C═N—C bond angles lying in the 170–180° range. For 2,6-xylenyl isocyanide, steric hindrance obviously plays an important role in making the C═N—C angles linear; however, structures d and f attribute the nature of the C═N and C—N bonds to sp and sp^2 character, respectively. So, in this case, electronic effects are also involved in the resulting structures of the complexes.

The 700–300-cm^{-1} Region. The Re–CO stretching and ReCO bending modes occur in this region. The most intense Raman peak at ~460 cm^{-1} is attributed to the symmetric $\nu(Re{-}CO)_{ax,eq}$ mode. Figure 2 shows Raman spectra for the $Re_2(CO)_{10-n}(CNBu\text{-}t)_n$ (n = 0–3) series. Clearly, the 460-cm^{-1} peak shifts to higher energy with increasing values of n, in accord with the σ-donor and π-acceptor properties of isocyanide ligands. Moreover, the Raman intensity in this region is comparable to that of the ν(CO) modes. Both regions can be used to probe the bonding properties of isocyanide ligands.

The 150–10-cm^{-1} Region. The strongest peak in the complete Raman spectra of the $Re_2(CO)_{10-n}(CNR)_n$ complexes is certainly the band located at ~120 cm^{-1}. Many years ago, this band was routinely assigned to the Re–Re stretching mode. But more recently, several different authors have presented a variety of spectroscopic arguments[20–22] to counter this assignment. Figure 7 shows a graph of wavenumber shift ($\Delta\nu$) for the 120-cm^{-1} band as a function of the degree of CNR substitution for different isocyanide ligands. A maximum is observed at approximately n = 2 (except for R = Me). If the Re–Re bond length is increasing regularly, it is quite reasonable to anticipate a monotonic decrease in ν(Re–Re). Crystallographic analysis[12] has demonstrated a steady increase in the Re–Re bond length with increasing value of n, while the UV spectra display a regular $\sigma \rightarrow \sigma^*$ red-band shift (Re–Re bond transition; $d_{z^2} \rightarrow d_{z^2}{}^*$).[31] So, Figure 7 is clear evidence that the 120-cm^{-1} band is not due to a pure Re–Re stretching mode. Adams et al.[18] have assigned this 120-cm^{-1} band to an antisymmetric CReC deformation mode. Upon successive substitution of CO groups by CNR ligands, this mode should then regularly increase in energy with increasing value of n. Again, Figure 7 partially disproves such an assignment. More likely, there is a very high degree of mixing of the Re–Re stretching and CReC deformation modes.

Acknowledgments. This research was generously supported by operating and equipment grants from the NSERC (Canada) and FCAR (Quebec). P.D.H. acknowledges the NSERC and McGill University (McConnell and Stewart Foundation) for graduate scholarships. We thank Z. H. Xu (Peking University) for technical assistance.

Registry No. $Re_2(CO)_{10}$, 14285-68-8; $Re_2(CO)_9(CNBu\text{-}t)$, 79138-90-2; $Re_2(CO)_8(CNBu\text{-}t)_2$, 79138-91-3; $Re_2(CO)_7(CNBu\text{-}t)_3$, 95590-06-0; $Re_2(CO)_9(CNC_6H_3Me_2)$, 95590-13-9; $Re_2(CO)_8(CNC_6H_3Me_2)_2$, 103774-03-4; $Re_2(CO)_7(CNC_6H_3Me_2)_3$, 103774-04-5; $Re_2(CO)_6(CNC_6H_3Me_2)_4$, 103774-05-6; $Re_2(CO)_9(CNCH_2Ph)$, 95590-07-1; $Re_2(CO)_8(CNCH_2Ph)_2$, 95590-08-2; $Re_2(CO)_7(CNCH_2Ph)_3$, 95590-09-3; $Re_2(CO)_9(CNMe)$, 95672-45-0; $Re_2(CO)_8(CNMe)_2$, 95590-17-3; $Re_2(CO)_7(CNMe)_3$, 95406-95-4.

Supplementary Material Available: Micro-Raman spectrum of $Re_2(CO)_{10}$ in the 2200–20-cm^{-1} region (Figure 1), data and proposed assignments for the FT-IR and micro-Raman spectra of $Re_2(CO)_{10-n}(CNR)_n$ (R = Bu-t, CH$_2$Ph, n = 1–3; R = C$_6$H$_3$Me$_2$-2,6, n = 1–4) (Tables II–IV), and low-energy micro-Raman spectra of $Re_2(CO)_{10-n}(CNCH_3)_n$ (n = 0–3) and micro-Raman spectra of $Re_2(CO)_{10-n}(CNR)_n$ (R = CH$_3$, CH$_2$Ph, n = 0–3; R = C$_6$H$_3$Me$_2$-2,6, n = 0–4) in the CO and CN stretching regions (Figures 4–6) (14 pages). Ordering information is given on any current masthead page.

---

(31) Butler, I. S.; Barreto, M. C.; Coville, N. J.; Harvey, P. D.; Harris, G. W., submitted for publication in *Inorg. Chem.*